

CHANNEL WAVEGUIDES

Prof. Alina Karabchevsky, www.alinakarabchevsky.com

Integrated Photonics Course 377-2-5599

School of ECE

Ben-Gurion University of the Negev, Israel

1

OUTLINES

Introduction

Waveguides types

- Slab waveguide
- Strip-loaded waveguide
- Ridge waveguide
- Rib waveguide
- Buried channel waveguide
- Diffused waveguide

Figure of merit

Probing an overtone with waveguides

Packaged Photonic Light Circuits

- PLC components
- H.W.

THE MOTIVATION

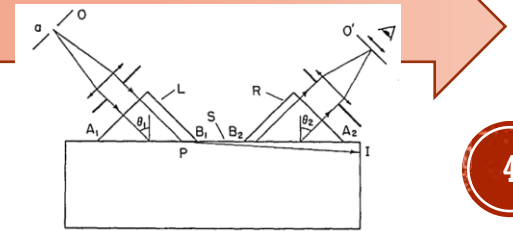
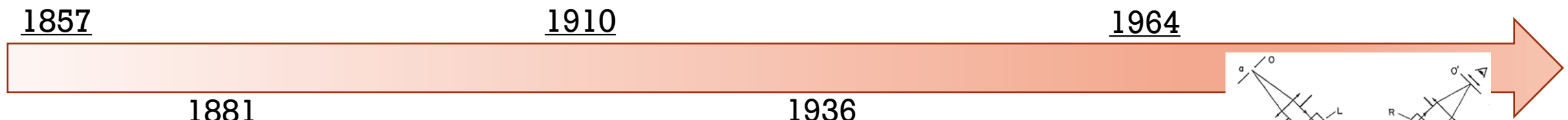
- Since the development of the laser in the early 1960s, guided wave optics has attracted much of interest.
- Experimental study shows that a waveguide can be efficiently utilized to detect the molecular overtones and to study their molecular dynamics.
- In Katiyi, A., Karabchevsky, A., Lightwave Technology (2017) figure-of-merit (FoM) is proposed for straight planar waveguides, minimized waveguides, and microfibers; then, it used to compare and assess most common waveguide architectures and conventional microfibers for overtones sensing.

MICRO- AND NANO- OPTICS: HISTORICAL OVERVIEW



- Faraday, M. (1857). The Bakerian Lecture: Experimental Relations of Gold (And Other Metals) to Light. Phil. Trans. R. Soc. 147, 145–181.
- Wheeler, W. (1881). Apparatus for Lighting Dwellings or Other Structures. Morton, Pennsylvania: US Patent Office.
- Hondros, D., and Debye, P. (1910). Elektromagnetische Wellen an Dielektrischen Drähten. Ann. Phys. 337 (8), 465–476.
- Carson, J. R., Mead, S. P., and Schelkunoff, S. A. (1936). Hyper-Frequency Wave Guides-Mathematical Theory. Bell Syst. Tech. J. 15 (2), 310–333.
- Osterberg, H., and Smith, L. W. (1964). Transmission of Optical Energy along Surfaces: Part II, Inhomogeneous Media. J. Opt. Soc. Am. 54, 1078.

$$\nabla \times \mathbf{H} = \frac{\partial \mathbf{D}}{\partial t} + \mathbf{J} \quad \nabla \cdot \mathbf{D} = \rho_{ext} + \gamma \frac{\partial \mathbf{D}}{\partial t}$$



from Integrated Photonics course lectures by A. Karabchevsky

WAVEGUIDES TYPES

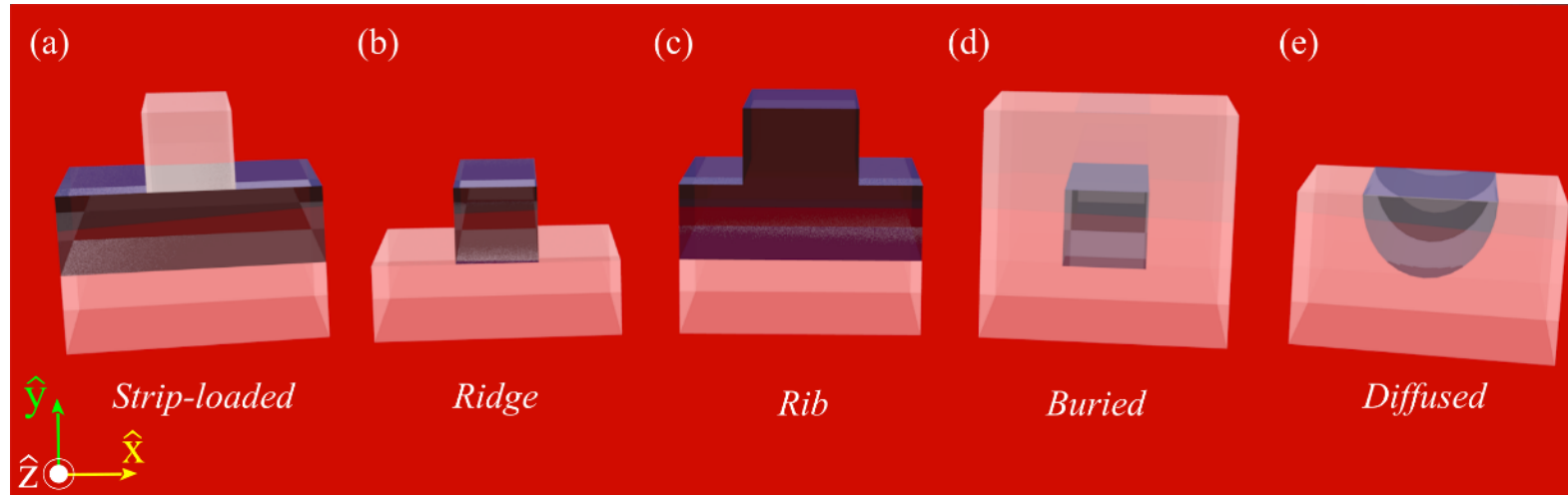


Figure 1: Common laterally confined passive waveguide structures: (a) a strip-loaded waveguide, (b) a ridge waveguide, (c) a rib waveguide, (d) a buried waveguide, and (e) a diffused waveguide. [Katiyi and Karabchevsky, J. Light. Technol., 2017]

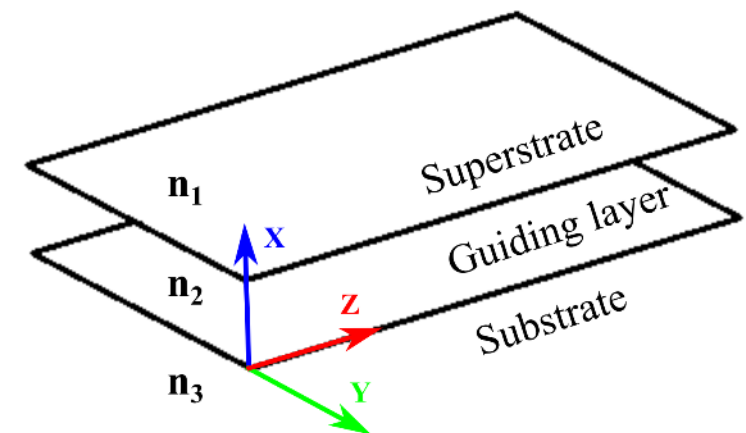
SLAB WAVEGUIDE

- The slab waveguide is modeled as a guiding layer, which is located above the substrate layer. The guiding layer is infinite at the y -plane.
- The mode confines only in the x -plane.

The height required for single-mode waveguide is:

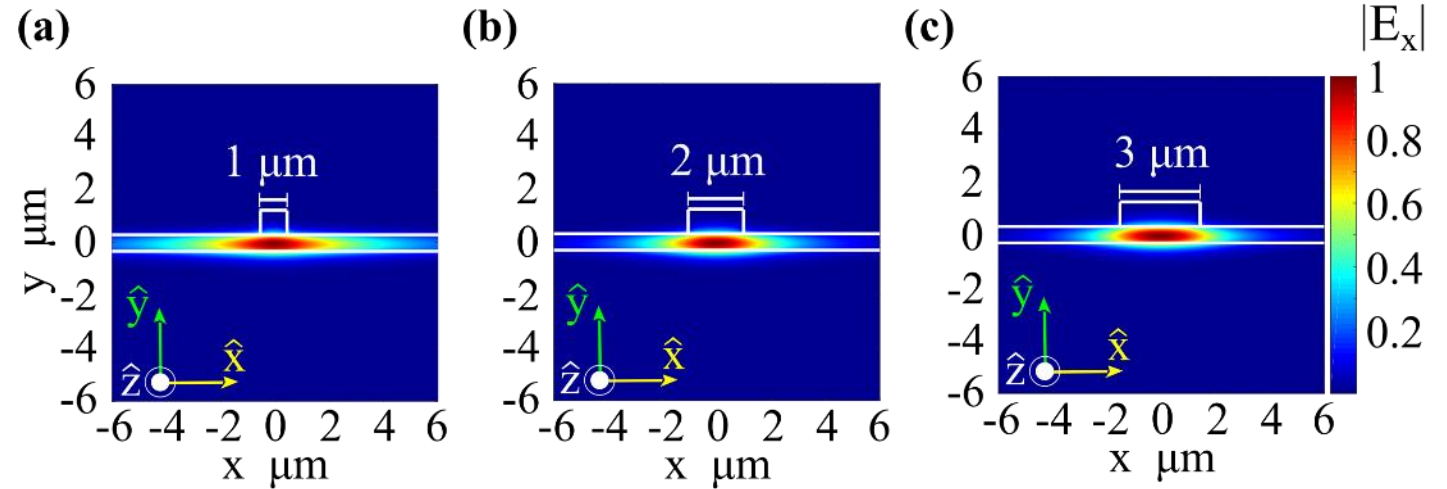
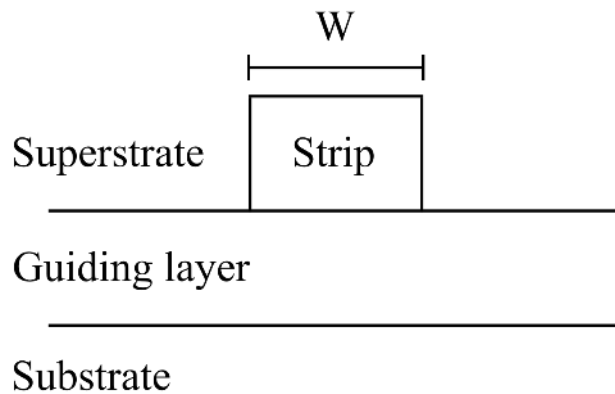
$$t_g < \frac{\lambda_0}{2\sqrt{n_1^2 - n_2^2}} \quad (1)$$

Where λ_0 is the wavelength in a vacuum.



STRIP-LOADED WAVEGUIDE

- To confine the mode in the y-plane, a metal or dielectric strip is placed on top of the slab waveguide. Increasing the strip width enhances the confinement.



STRIP-LOADED WAVEGUIDE

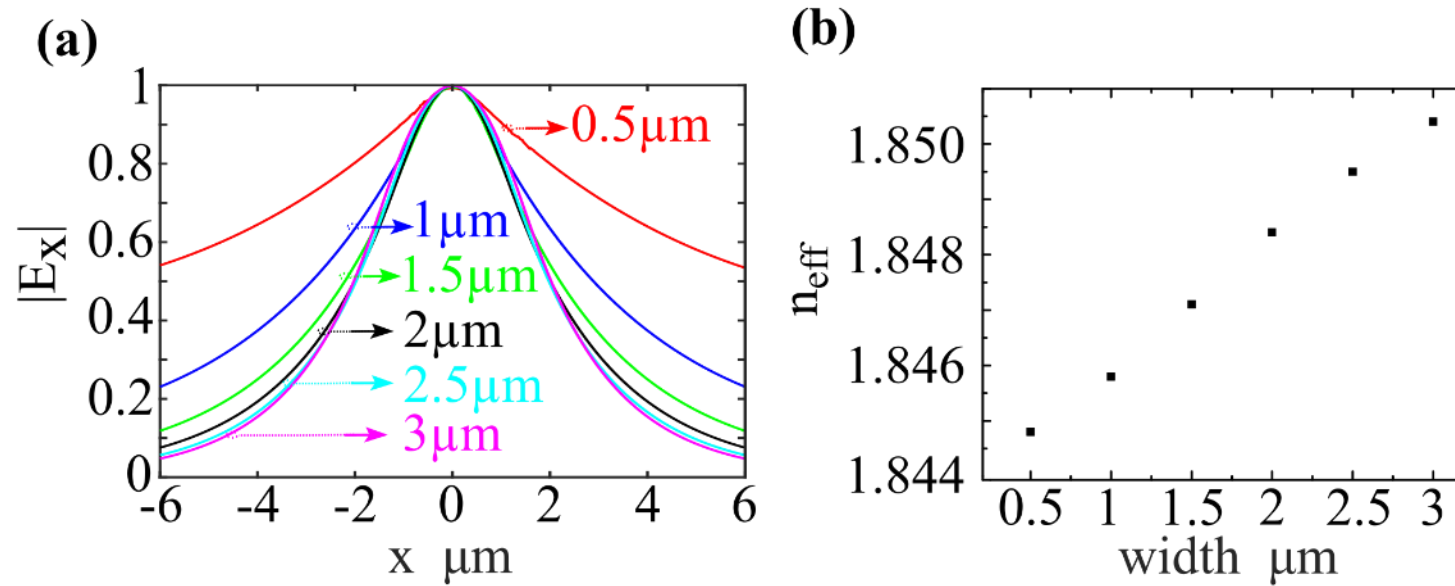
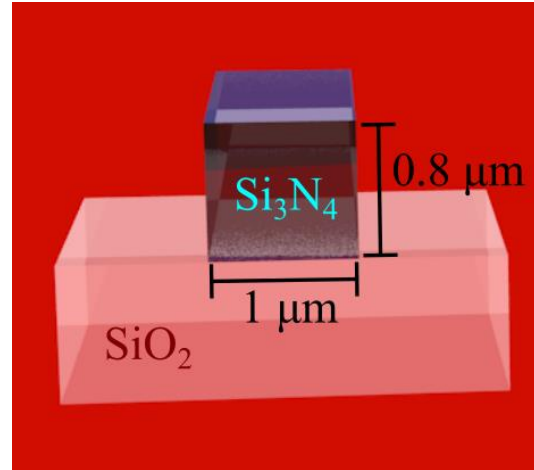


Figure 2: (a) The cross-section profiles. (b) The change in the effective index as function of the strip width [1].

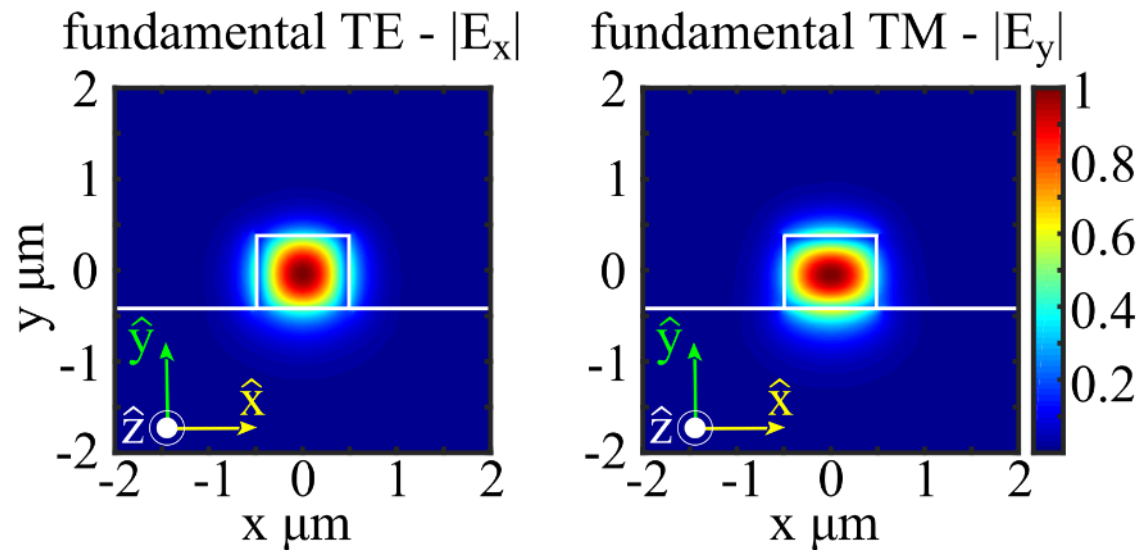
RIDGE WAVEGUIDE



- The guiding layer is made of high-index strip.
- The surrounding medium has a lower refractive index than that of the guiding layer, resulting in a higher confinement.

RIDGE WAVEGUIDE

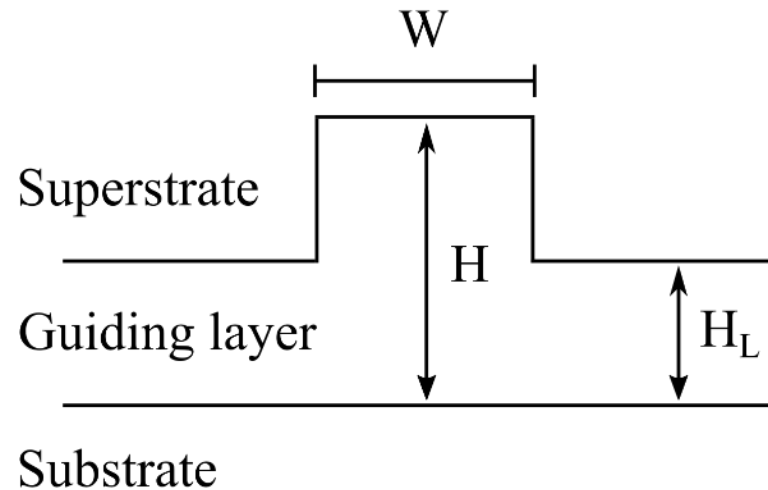
- TE fundamental mode has higher confinement since the waveguide core is embedded in low-index media (air) from both side in the x-plane [1].



SI OXYNITRIDE WAVEGUIDES

- Employs silica substrate but uses SiON for the core layer.
- SiON alloy is made by combining SiO_2 with Si_3N_4 , two dielectrics with refractive indices of 1.45 and 2.01.
- Refractive index of SiON layer can vary from 1.45-2.01.
- SiON film deposited using plasma-enhanced chemical vapor deposition (SiH_4 combined with N_2O and NH_3).
- Low-pressure chemical vapor deposition also used (SiH_2Cl_2 combined with O_2 and NH_3).
- Photolithography pattern formed on a 200-nm-thick chromium layer.
- Propagation losses are typically < 0.2 dB/cm.

RIB WAVEGUIDE



- Rib waveguide is very similar in appearance to the strip-loaded waveguide. The strip is made of the same material as that of the guiding layer.
- Consequently, the guiding layer has two different height areas.
- Since the fundamental mode has less contact with edges due to its guiding layer shape, a rib waveguide exhibits lower scattering loss.

RIB WAVEGUIDE

Assuming the rib structure equation for a single operation yields:

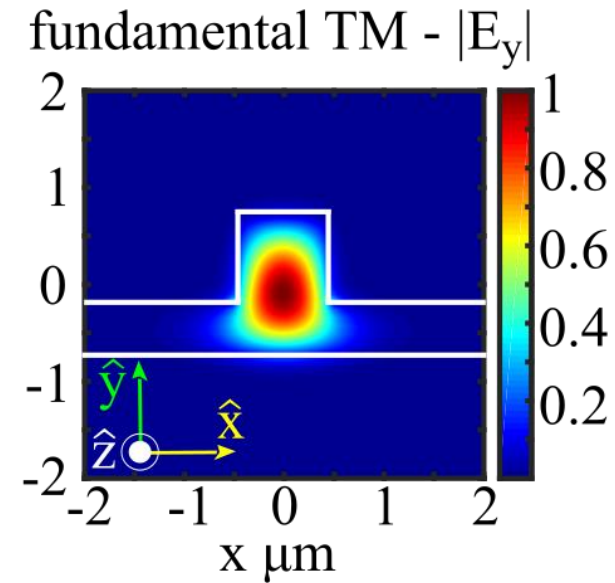
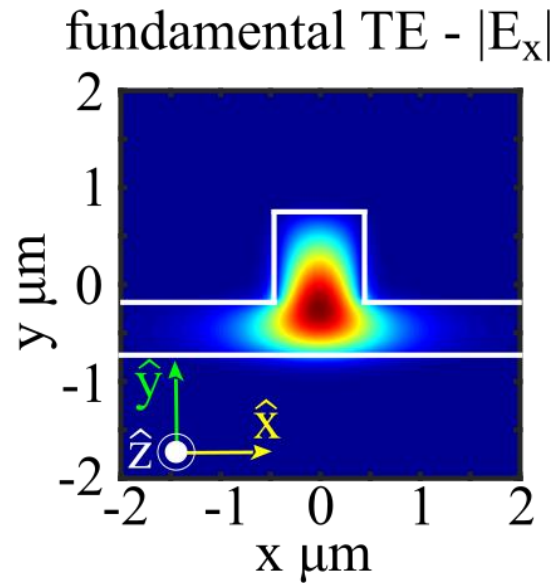
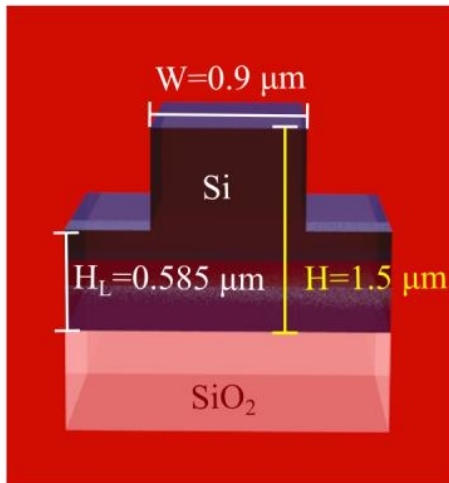
$$\frac{W}{H} = 0.3 + \frac{r}{\sqrt{1-r^2}} \rightarrow r \geq 0.3 \quad (2)$$

$$H_L = rH \quad (3)$$

Where W is the rib width, H is the height and H_L is the height of the slab film.

- By adjusting the height and width of the strip, a single-mode rib waveguide can be bigger compared to a ridge waveguide made of the same materials.
- It makes the coupling easier - the main advantage of this structure.

RIB WAVEGUIDE FUNDAMENTAL MODES



- It shows that the fundamental mode has lower interaction with edges [1].

SILICON-ON-INSULATOR - STRUCTURE

- If the geometry of the rib waveguide is correctly designed, higher-order modes leak out of the waveguide over a very short distance, leaving only the fundamental mode propagating.
- The effective index of 'vertical modes' in the planar region each side of the rib becomes higher than the effective index of all vertical modes in the rib, other than the fundamental.
- Thus, all modes other than the fundamental vertical mode are cut off.
- Intuitively this seems reasonable as the second vertical mode in the rib will have an electric field profile with two peaks, the latter overlapping well with the fundamental mode of the planar region adjacent to it, and hence coupling to it.

PROGRESSION OF A HIGHER-ORDER MODE

- The first figure represents the launch conditions, deliberately off-center in order to excite higher-order modes.
- The second diagram shows waveguide modes after travelling 250 μm , which clearly exhibit more than a single mode.
- After 2000 μm the mode profile is essentially that of only the fundamental mode.

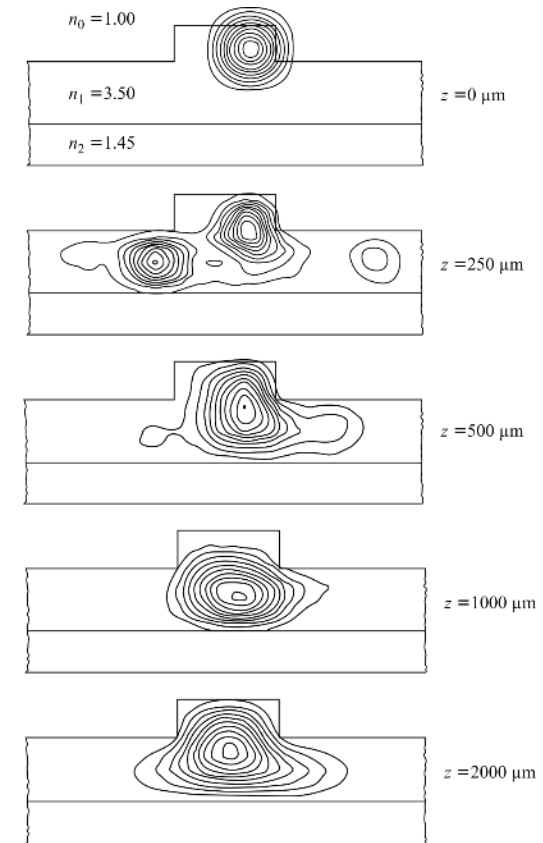
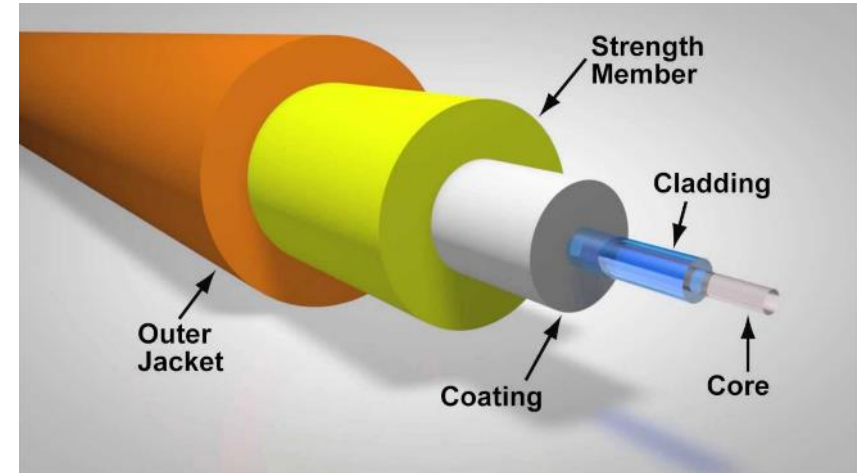


Figure 3: Propagation simulation of a rib waveguide.

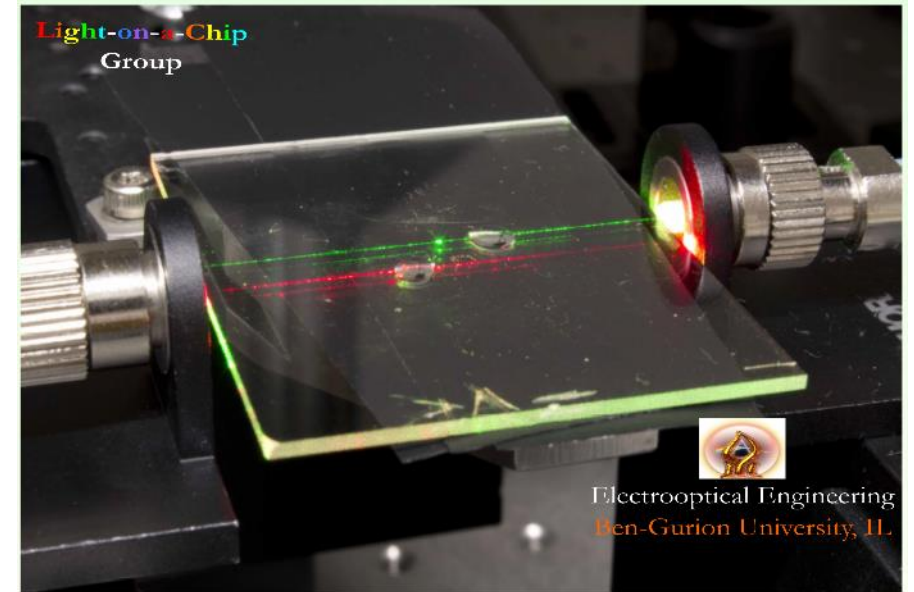
BURIED CHANNEL WAVEGUIDE

- The guiding layer is surrounded by a dielectric material with a lower refractive index.
- The most common configuration of the buried waveguide is fiber, as its flexibility, low propagation losses (0.2 dB/km for a 1.55 μm single mode fiber (SMF)), and low price makes it adequate for transferring communication and data over long distances.
- Although it results in an optically weak waveguide, this structure is advantageous due to the affordability of silica and the simplicity of fabrication.



DIFFUSED WAVEGUIDE

- The fabrication process involves ion-exchange between the salt and glass which increases the refractive index.
- The substrate layer of a diffused-channel waveguide is made of materials such as soda lime glass, Pyrex, Corning 3-71, or borosilicate (BK7).
- The main advantage of an ion-exchange waveguide is its low propagation losses, although its structure is an optically weak ($\Delta = 0.5\%$ in BK7, using KNO_3).



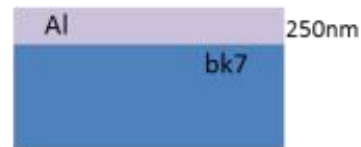
DIFFUSED WAVEGUIDE FABRICATION PROCESS

1. Cleaning

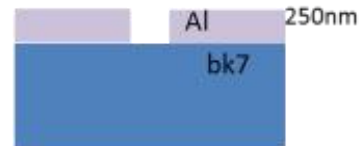


Acetone
IPA
Blow/Rinse with Water

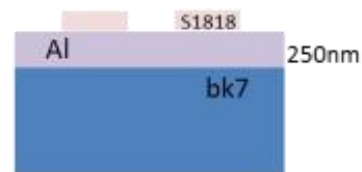
2. Al mask deposition by Vacuum evaporation



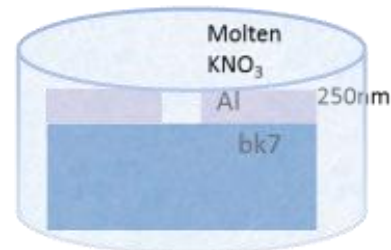
5. Al etch



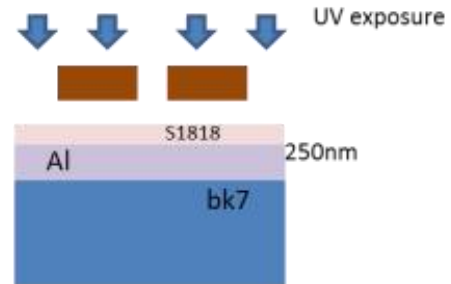
4. Resist removal with SVC-14



6. Immersion in KNO_3 for at 395°C for 11hr



3. Positive photolithography



7. Sawing/Lapping/Polishing



5 mm from each side

Appropriate holding jig

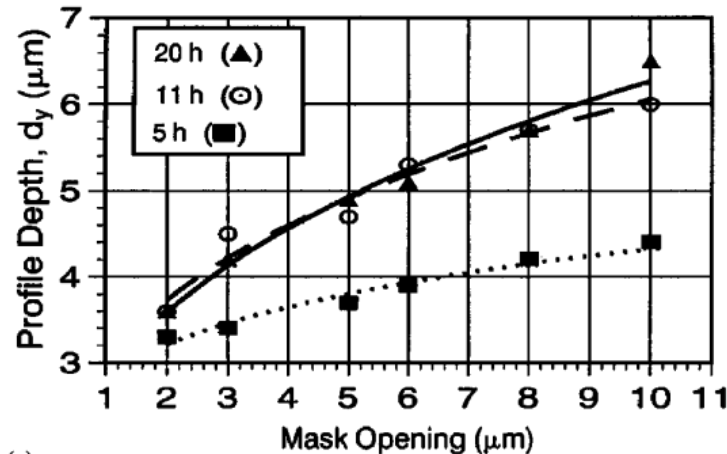


Appropriate Lapping/polishing jig

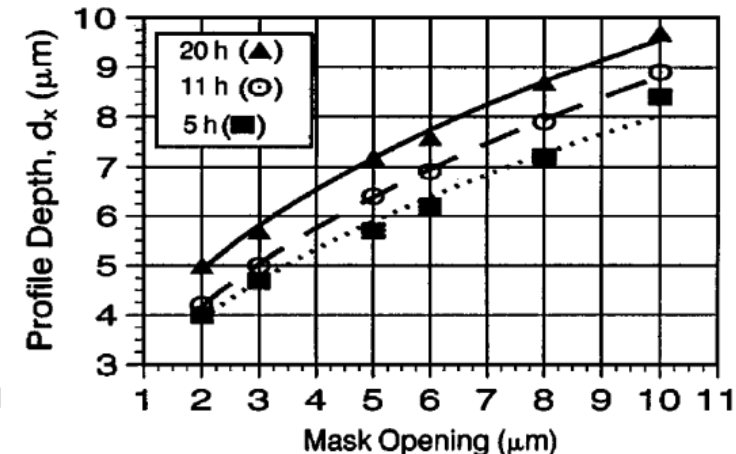


DIFFUSED WAVEGUIDE: FABRICATION

- 1) The mask opening and the baking time define the penetration depth and width of the ion-exchange [2].



(a)



(b)

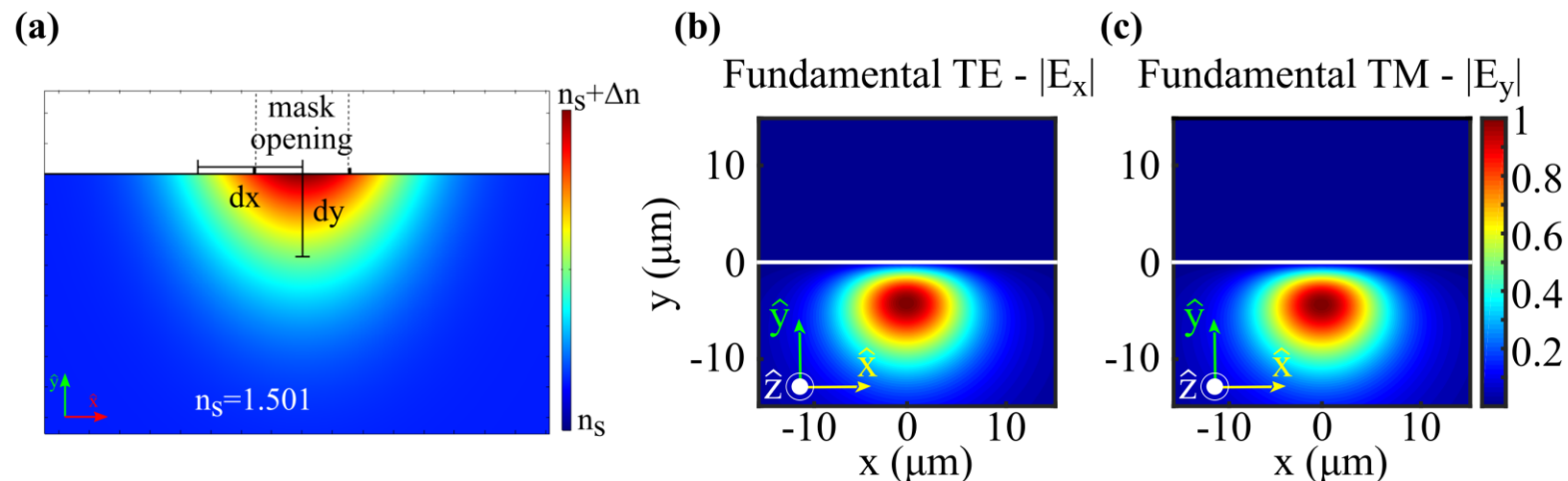
- 2) The type of ions implanted inside the glass defines the optical properties of the core, Δn . For example, $\Delta n = 0.009$ for KNO_3 and $\Delta n = 0.028$ for AgNO_3 .

DIFFUSED WAVEGUIDE

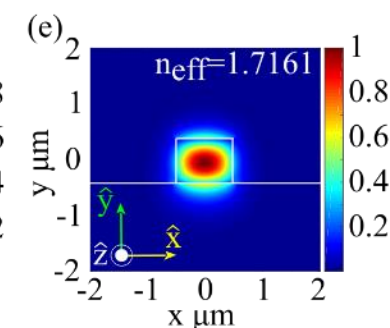
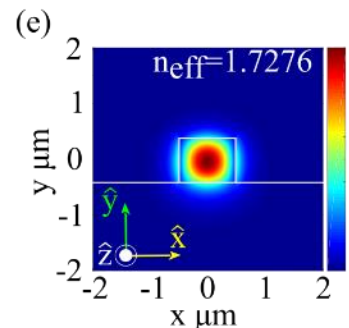
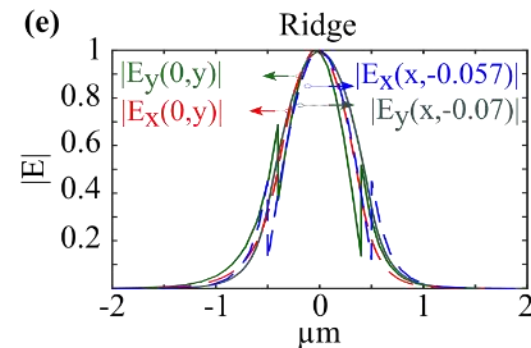
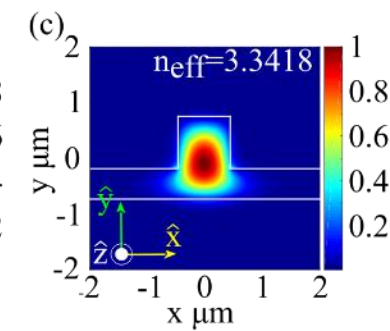
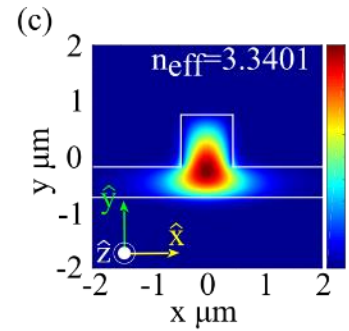
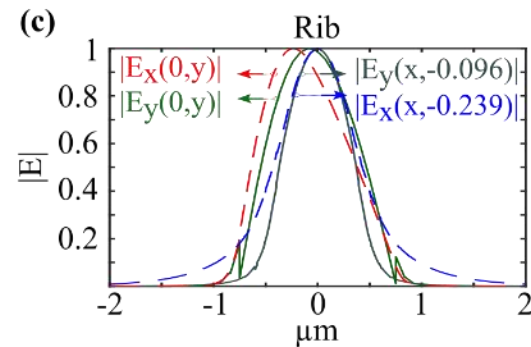
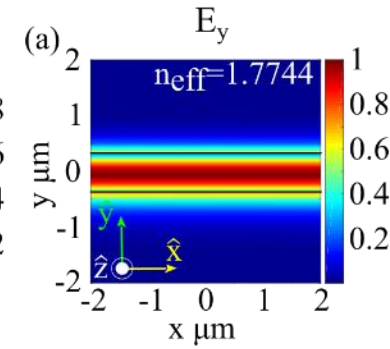
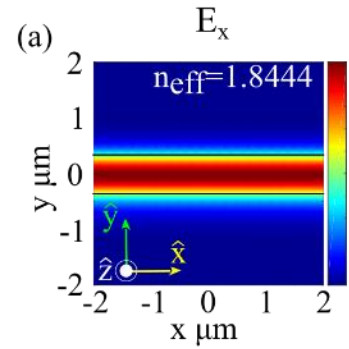
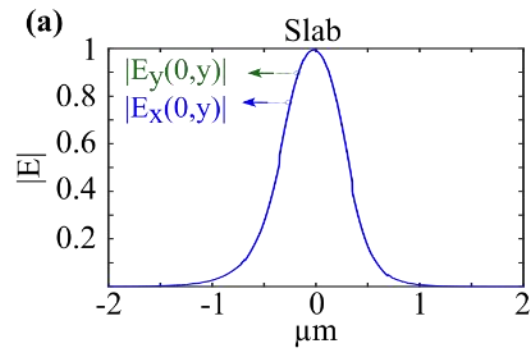
As the fabrication process involves ion-exchange, the refractive index varies non-linearly:

$$n(x, y) = n_s + \Delta n \cdot \operatorname{erfc}\left(\frac{y}{dy}\right) \exp\left(\frac{-x^2}{dx^2}\right) \quad (4)$$

Where n_s is the refractive index of substrate, dx and dy are the penetration depths in x and y axis respectively, and Δn is the maximal index change [1].



CROSS-SECTION OF FUNDAMENTAL MODES



CROSS-SECTION OF FUNDAMENTAL MODES

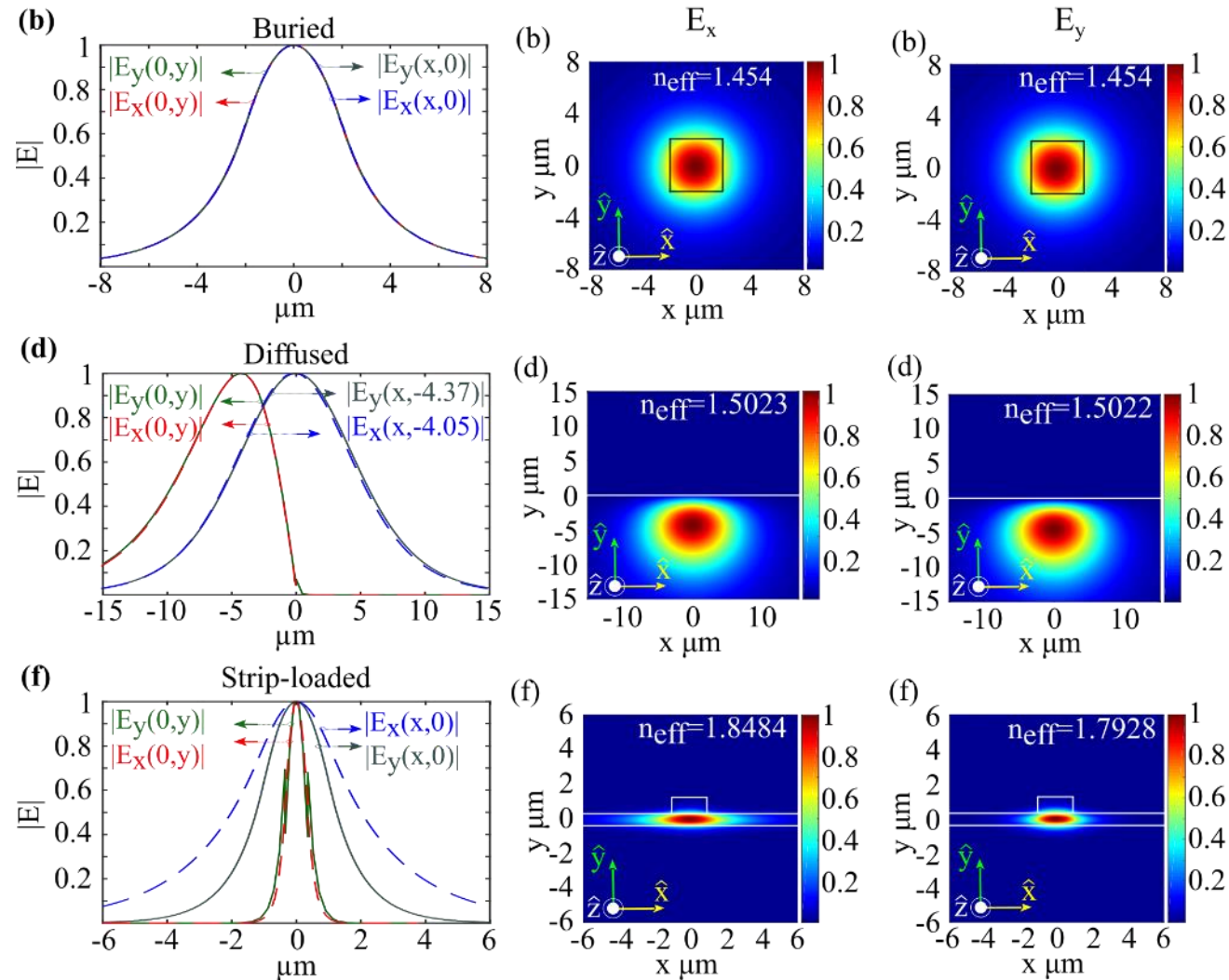


FIGURE OF MERIT FOR SENSING APPLICATIONS

FoM is the fraction of the power carried by the evanescent tail as shown in Eq. (5). The fraction of the power in the guiding layer is shown in Eq. (6).

$$\text{FoM} = \eta_{\text{evan}} = \frac{P_{\text{evan}}}{P_{\text{total}}} = \frac{\int_{\text{sup}} S dA}{\int_{-\infty}^{\infty} S dA} \quad (5)$$

$$\eta_{\text{core}} = \frac{P_{\text{core}}}{P_{\text{total}}} = \frac{\int_{\text{core}} S dA}{\int_{-\infty}^{\infty} S dA} \quad (6)$$

Where η is the fraction of the power, P is the power, A is the area and S is the time varying Poynting vector defined as:

$$S = \frac{1}{2} \Re\{E \times H^*\}$$

Where E is the electric field vector, H is the magnetic field vector and \Re is the real part.

FOM FOR SINGLE-MODE WAVEGUIDE EMBEDDED IN AIR

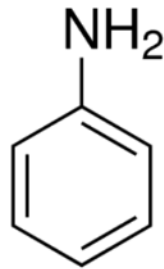
- We calculated the FoM for single-mode waveguide embedded in air [1].

Table 1: Fraction of the power propagating in single-mode waveguides embedded in air

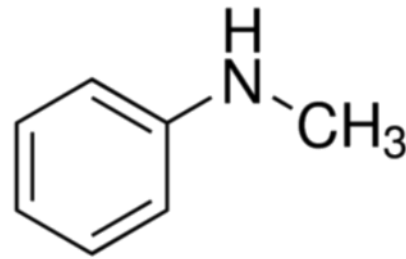
Waveguide type	Quasi-TE		Quasi-TM	
	η_{core}	FoM	η_{core}	FoM
Ridge	0.909	0.036	0.895	0.041
Slab	0.912	0.028	0.899	0.016
Rib	0.992	0.003	0.993	0.006
Diffused	0.999	0.0001	0.999	5.18E-05
Strip	0.904	0.013	0.886	0.004

THE PROBING ANALYTE

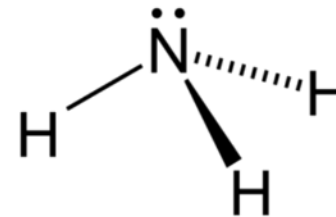
(a)



(b)



(c)



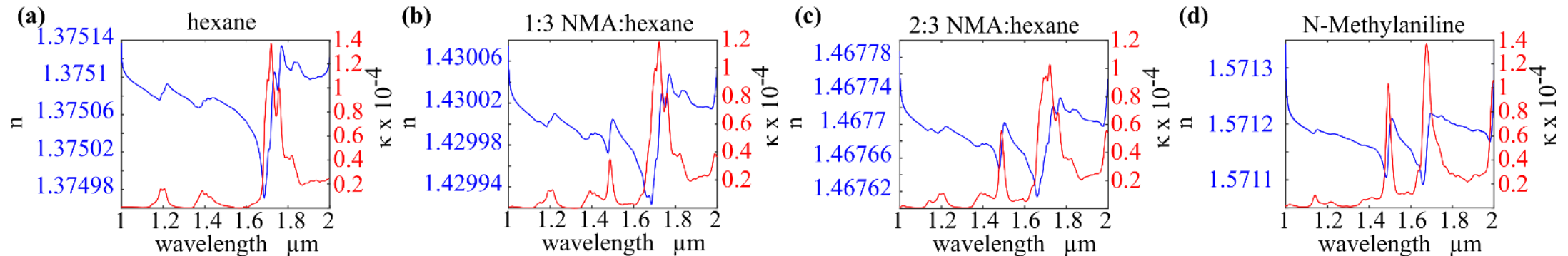
- We use the amine-based molecule NMA as a probe molecule to demonstrate the concept of probing molecular overtones with guided-wave optics in the near-infrared.
- We evaluated the extinction coefficient (κ) from the measured absorption by using a cuvette with a 1 mm path length.

KRAMERS-KRONING (KK) RELATION

- The index n calculated using the Kramers-Kroning (KK) relation implemented in Matlab with the Hilbert transform:

$$n(\omega) - 1 = \frac{2}{\pi} \mathcal{P} \int_0^{\infty} \frac{\omega' \kappa(\omega')}{(\omega'^2 - \omega^2)} d\omega' \quad (7)$$

Where \mathcal{P} is the Cauchy principal value and ω is the angular frequency.



DISPERSION ANALYSIS

- To model waveguides embedded in index of refraction related to the mixture ratio 1:3 of N-Methylaniline to hexane which is:

$$n(\lambda = 1.496 \mu m) = 1.4299855 + j2.66917 \times 10^{-6}$$

- Mixture ratio 1:3 of N-Methylaniline to hexane was chosen to support the single-mode propagation in a silica fiber.
- The FoM was calculated for single-mode dimensions of waveguide that was calculated when embedded in air.
- Rather than the buried waveguide, one can consider an optical fiber.

FOM FOR SINGLE-MODE WAVEGUIDES EMBEDDED IN THE MIXTURE

- We calculated the FoM for single-mode waveguide embedded in mixture [2].

Table 2: Fraction of the power propagating in single-mode waveguide embedded in mixture ratio 1:3 of N-Methylaniline to hexane

Waveguide type	Quasi-TE		Quasi-TM	
	η_{core}	FoM	η_{core}	FoM
Ridge	0.868	0.087	0.859	0.094
Slab	0.896	0.051	0.883	0.056
Rib	0.991	0.004	0.992	0.007
Diffused	0.998	0.002	0.998	0.002

INTERACTION ENHANCEMENT

- Minimizing the guiding layer is an elegant approach to increase the evanescent field and strengthen the interaction with the analyte.
- We minimized the guiding layer while still considering the practical fabrication limitations. For example, rib and ridge structures can be tapered only in the x -plane.
- We provide a systematic comparison between different waveguide architectures by minimizing the physical dimensions of the structures with the same rate (in our case 50%).

TAPERED WAVEGUIDES

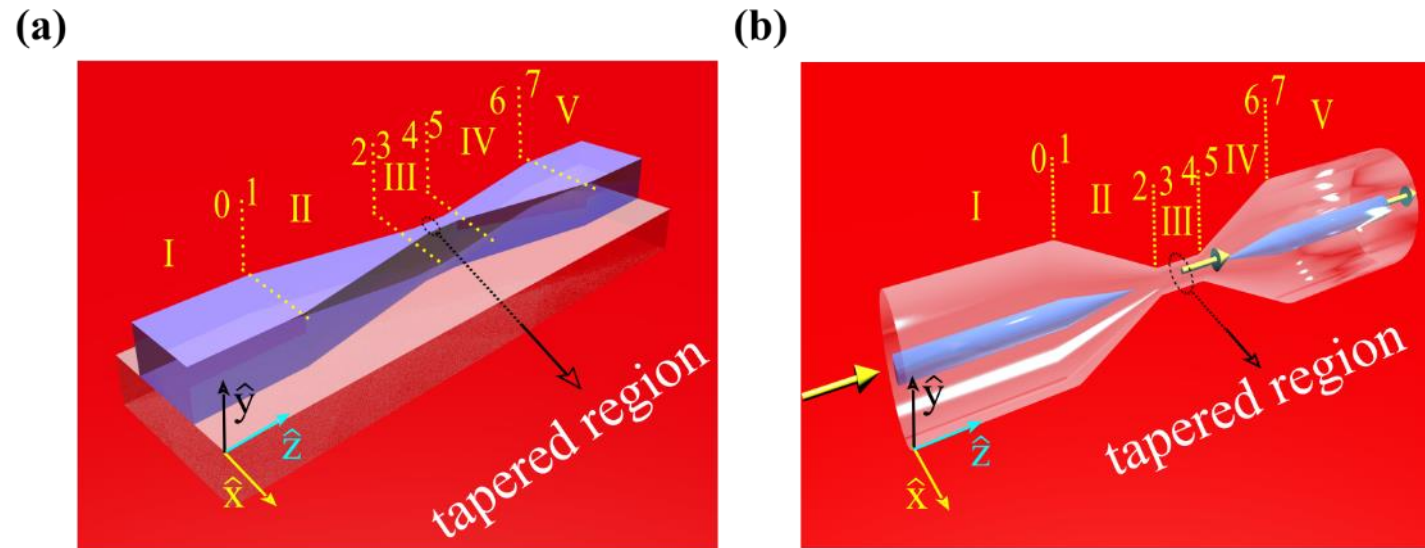


Figure 4: Examples of tapered waveguide structures: (a) tapered ridge waveguide, (b) micro-fiber.

FOM FOR MINIMIZED CORE WAVEGUIDES EMBEDDED IN THE MIXTURE

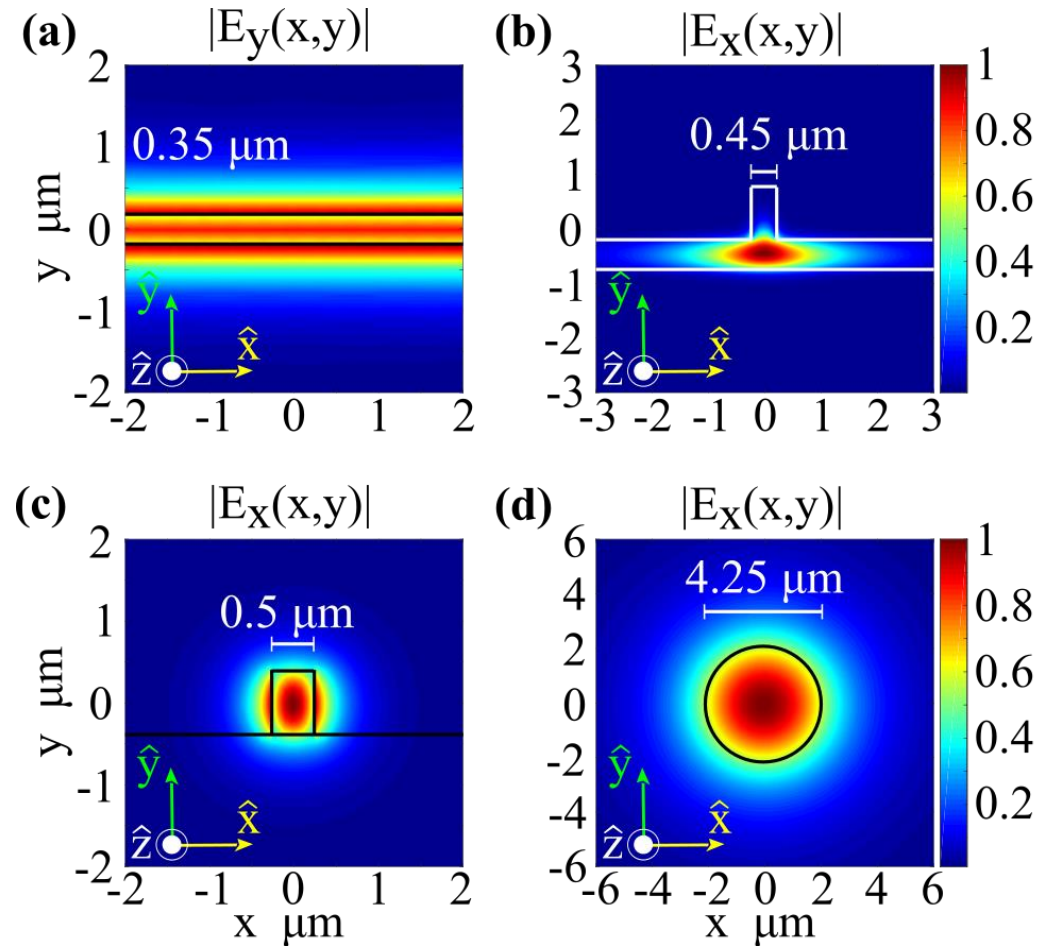
Table 3: Fraction of the power carried by the modes of minimized waveguides embedded in molecular mixture.

Waveguide type		
	η_{core}	FoM
Ridge	0.598	0.323
Rib	0.978	0.011
Fiber	0.671	0.329

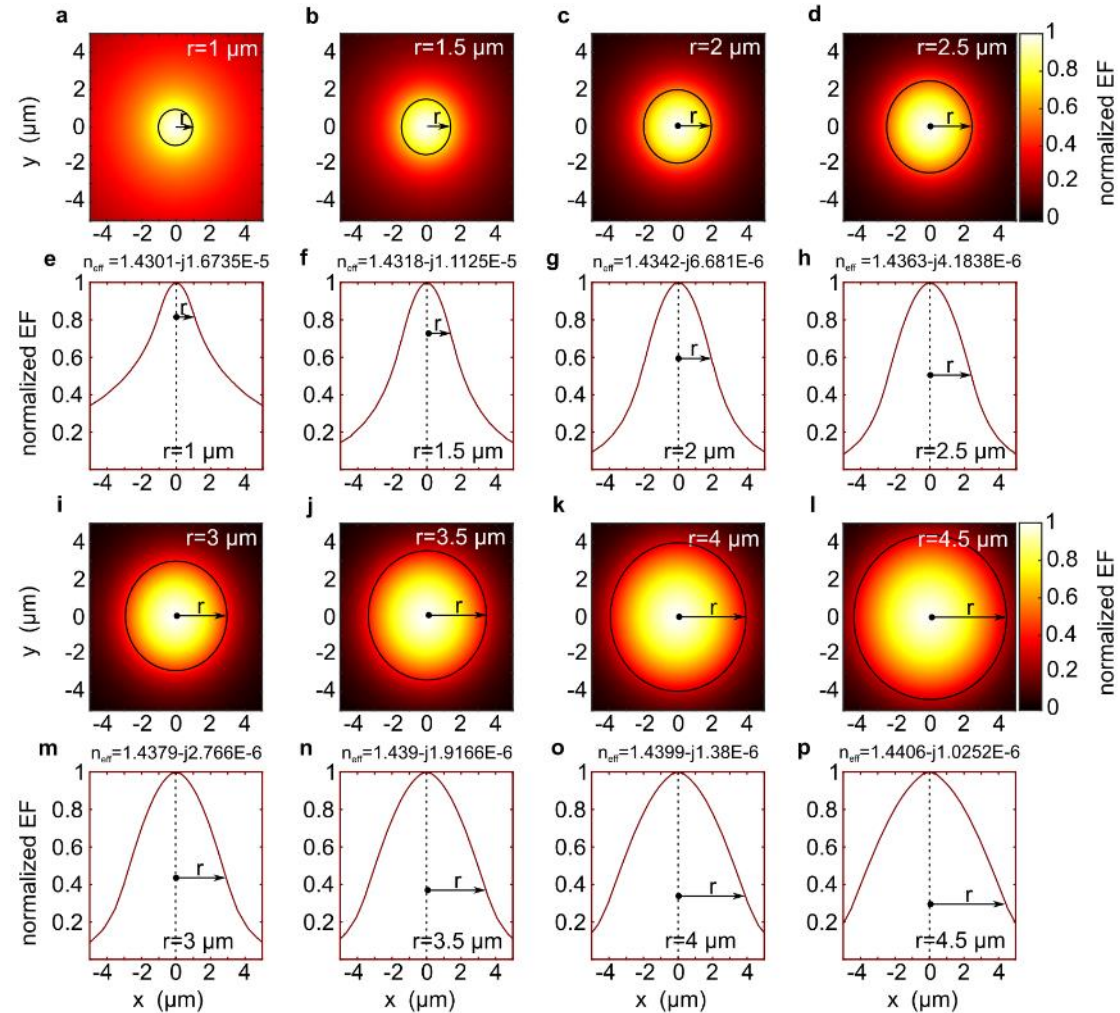
- The minimizing of the structure can be seen to increase the FoM, as compared with the values summarized in Table 2.
- The ridge waveguide and the fiber show the highest FoM values, which is more than 30%.

MODES IN MINIMIZED CORE WAVEGUIDES

- Minimizing the physical dimensions of the structures leads to increased evanescent field amplitudes in the superstrate compared to single-mode waveguide.



MODES IN MINIMIZED FIBER



CROSS-SECTIONS OF THE EVANESCENT TAIL IN MINIMIZED WAVEGUIDES

- The amplitude and the penetration depth of the evanescent tail increase due to the minimizing of the guiding layer.

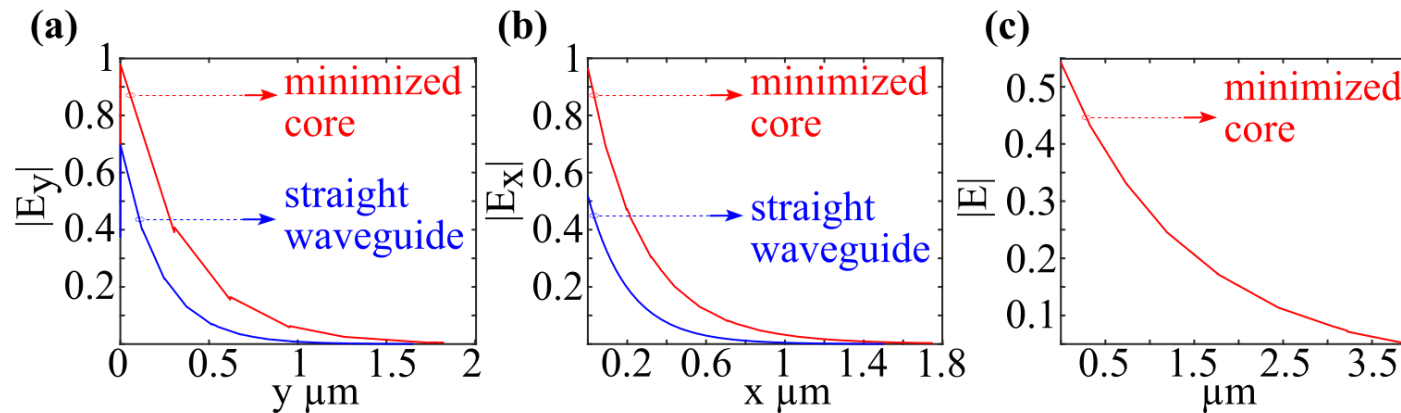


Figure 5: Cross-section of the evanescent tail in minimized waveguide compared to single-mode waveguides embedded in the mixture. (a) Slab waveguide, (b) Si_3N_4 ridge waveguide on silica, and (c) silica microfiber [1].

COMPARISON OF OPTICAL INTEGRATED CIRCUITS WITH ELECTRICAL INTEGRATED CIRCUITS

Advantages:

- Increased bandwidth.
- Expanded frequency (wavelength) division multiplexing.
- Low-loss couplers, including bus access types.
- Expanded multipole switching (number of poles, switching speed).
- Smaller size, weight, lower power consumption.
- Batch fabrication economy.
- Improved reliability.
- Improved optical alignment, immunity to vibration.

Major disadvantage

- High cost of developing new fabrication technology.

CMOS/PHOTONIC CIRCUIT

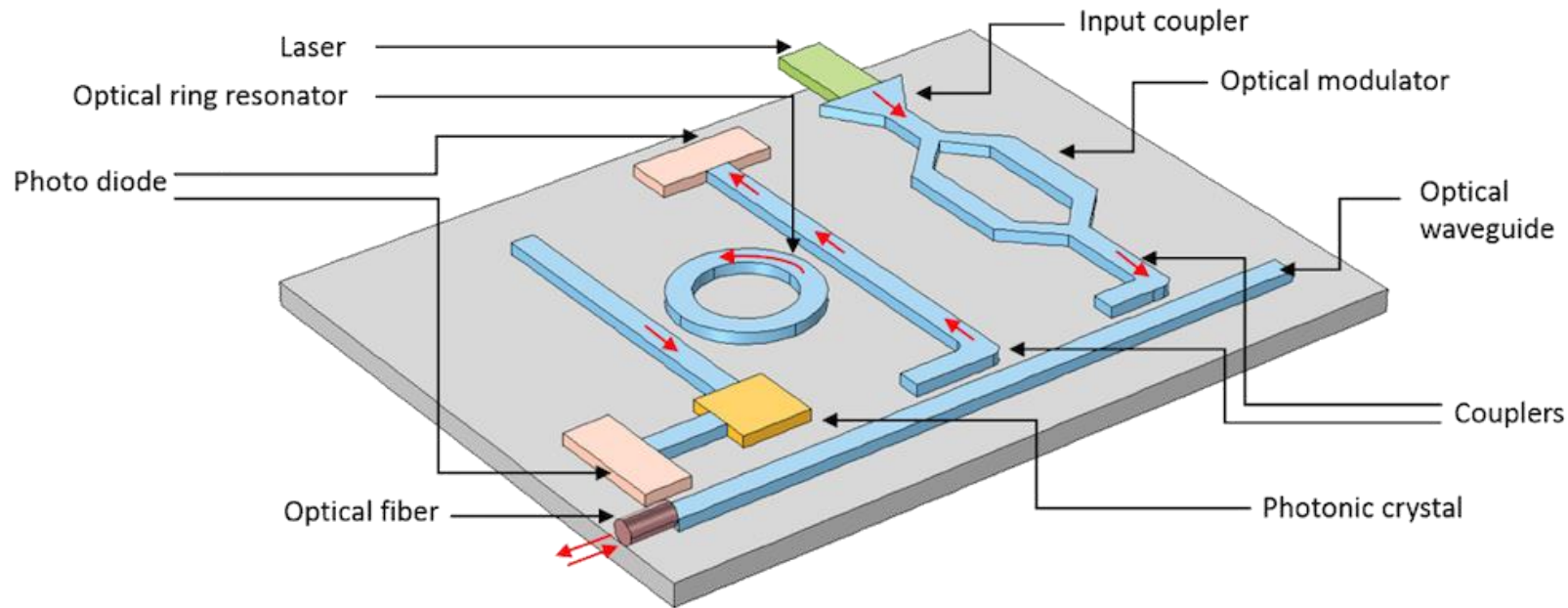


Figure 6: Conceptualization of a CMOS/photonic circuit. Silicon photonic-electronic circuits can support systems with hundreds or thousands of such components today [from Comsol].

PACKAGED PHOTONIC LIGHT CIRCUITS (PLC)

- Package design for minimizing insertion losses.
- Fibers inserted into V-shaped grooves formed on a glass substrate.
- Glass substrate connected to the PLC chip using an adhesive.
- A glass plate placed on top of V grooves is bonded to the PLC chip.

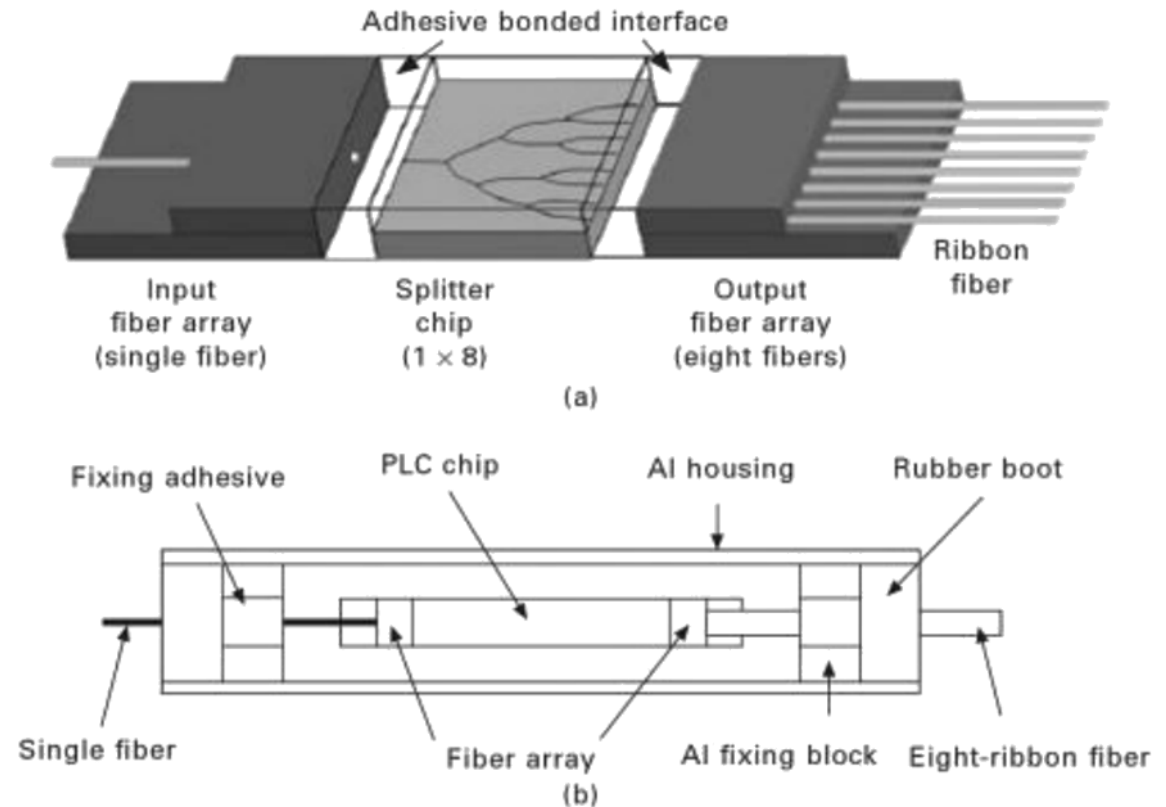


Figure 7: Packaged PLC.

PLC COMPONENTS

Passive components:

- Y and X junctions.
- Grating-assisted directional couplers.
- Mach-Zehnder filters.
- Multimode interference couplers.
- Star couplers.
- Arrayed-waveguide gratings.

Active components:

- Semiconductor lasers and amplifiers.
- Optical modulators.
- Photodetectors.

INTEGRATED PHOTONIC CIRCUITRY

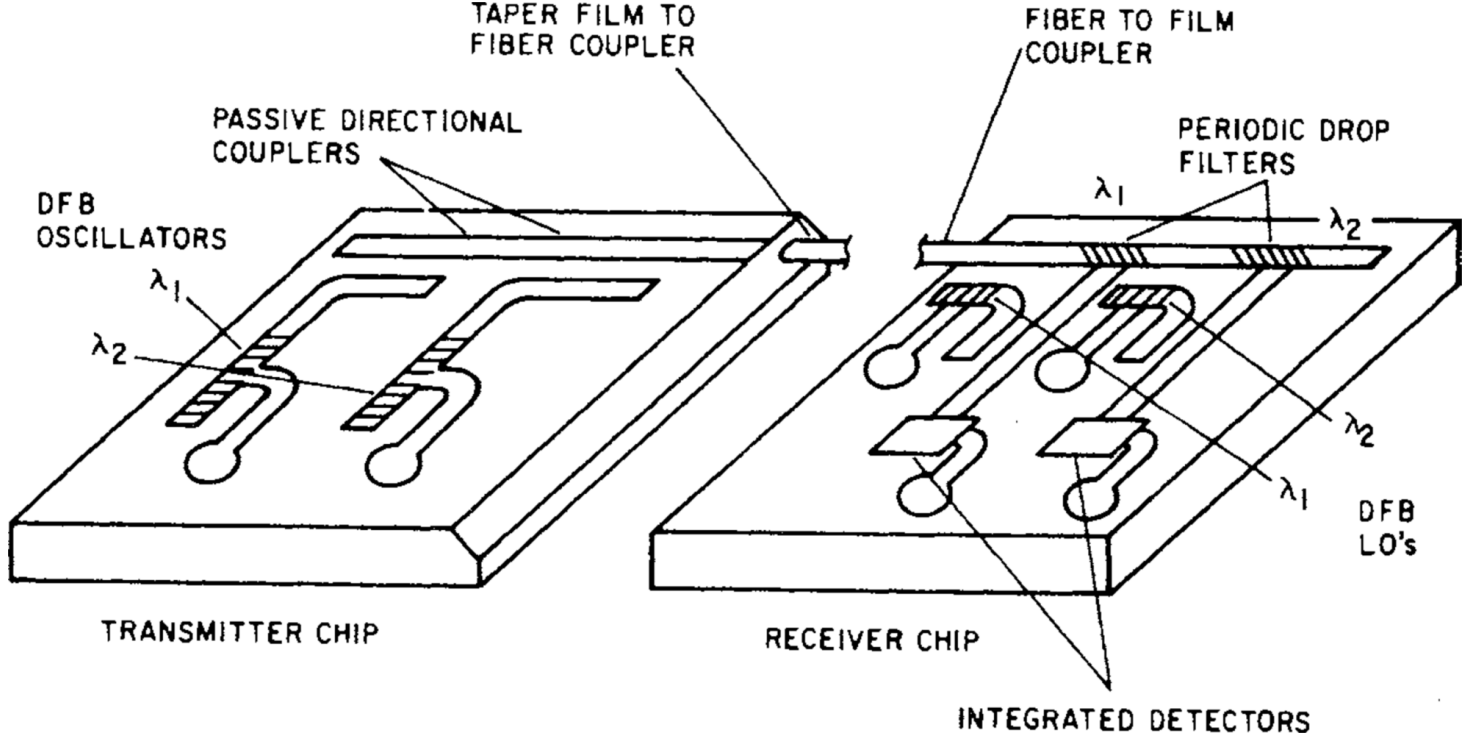


Figure 8: Monolithic integrated optic system for optical communications.

Y JUNCTIONS

A device that acts as a power divider, made by splitting a planar waveguide into two branches bifurcating at some angle θ .

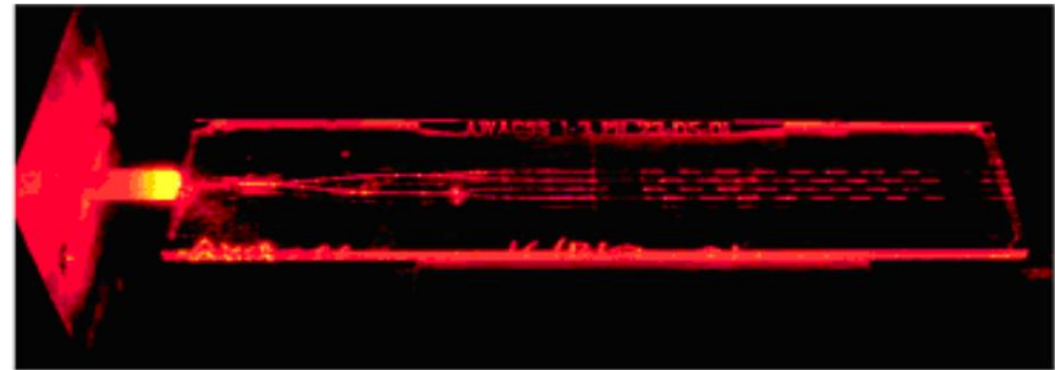
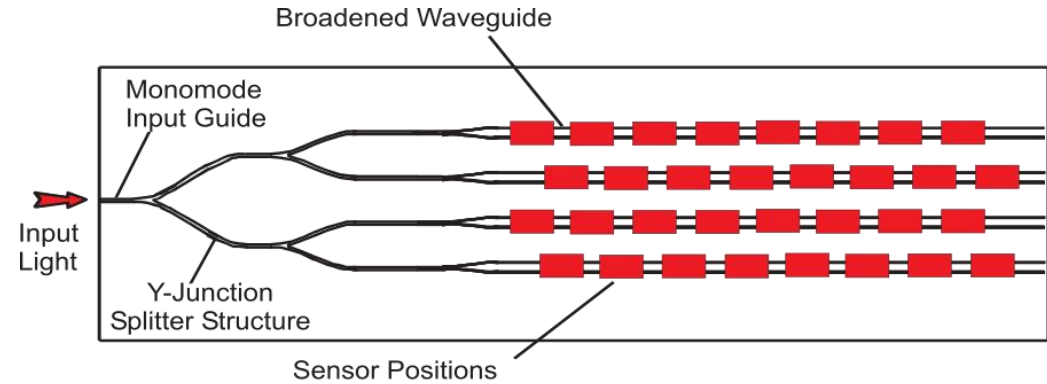


Figure 9: Multisensor, from Ping Hua et al. Opt Express 13(4), 2005.

BRANCHING ANGLE θ IN STRAIGHT BEND

- No coupling region exists in which modes of different waveguides overlap.
- In the junction region, waveguide is thicker and supports higher order modes and the power is divided into two branches.
- Sudden opening of the gap violates adiabatic condition, resulting in some insertion losses for any Y junction.
- Losses depend on branching angle θ and increase with it. θ should be below 1° to keep insertion losses below 1 dB.

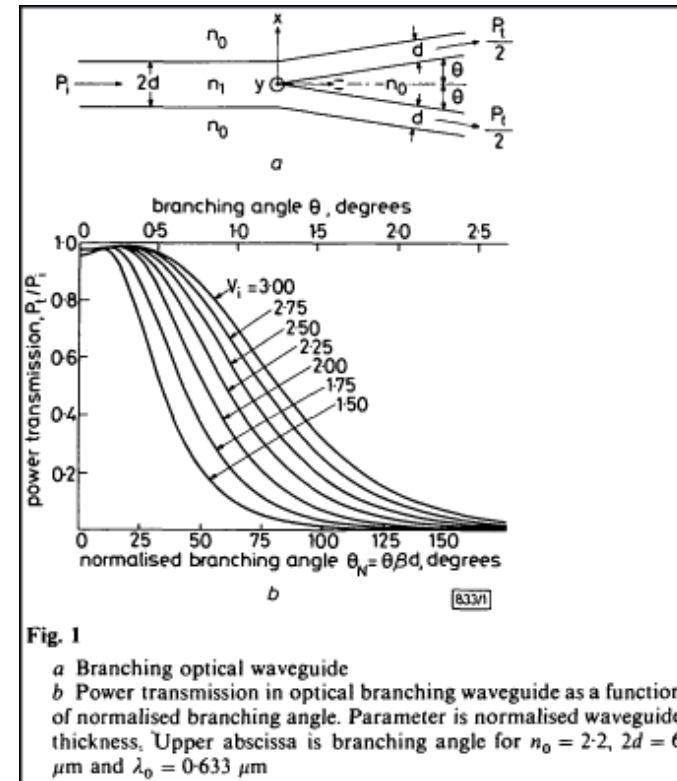


Fig. 1
a Branching optical waveguide
b Power transmission in optical branching waveguide as a function of normalised branching angle. Parameter is normalised waveguide thickness. Upper abscissa is branching angle for $n_0 = 2.2$, $2d = 6 \mu\text{m}$ and $\lambda_0 = 0.633 \mu\text{m}$

Figure 10: Branching optical waveguides, from Electronics Letters 17(3), 1981.

POWER TRANSMISSION IN Y SPLITTER WITH STRAIGHT BEND

Power is obtained as an overlap integral between incident and transmitted fields.

- Power transmission of TE waves

$$\frac{P_t}{P_i} = \left| \frac{\beta}{2\omega\mu_0} \int_{-\infty}^{\infty} E_{yi} E_{yt} dx \right|^2$$

where E_{yi} and E_{yt} as defined in Electronics Letters 17(3), 1981.

X JUNCTIONS FOUR-PORT COUPLERS

- Spacing between waveguides reduced to zero in coupled Y junctions.
- Waveguides cross in the central region in a X coupler.
- In asymmetric X couplers, two input waveguides are identical but output waveguides have different sizes.
- Power splitting depends on relative phase between two inputs.
- If inputs are equal and in phase, power is transferred to the wider core; when inputs are out of phase, power is transferred to narrow core.



Figure 11: Fiber coupler [from Thorlabs].

FOUR-PORT COUPLERS: WAVEGUIDES

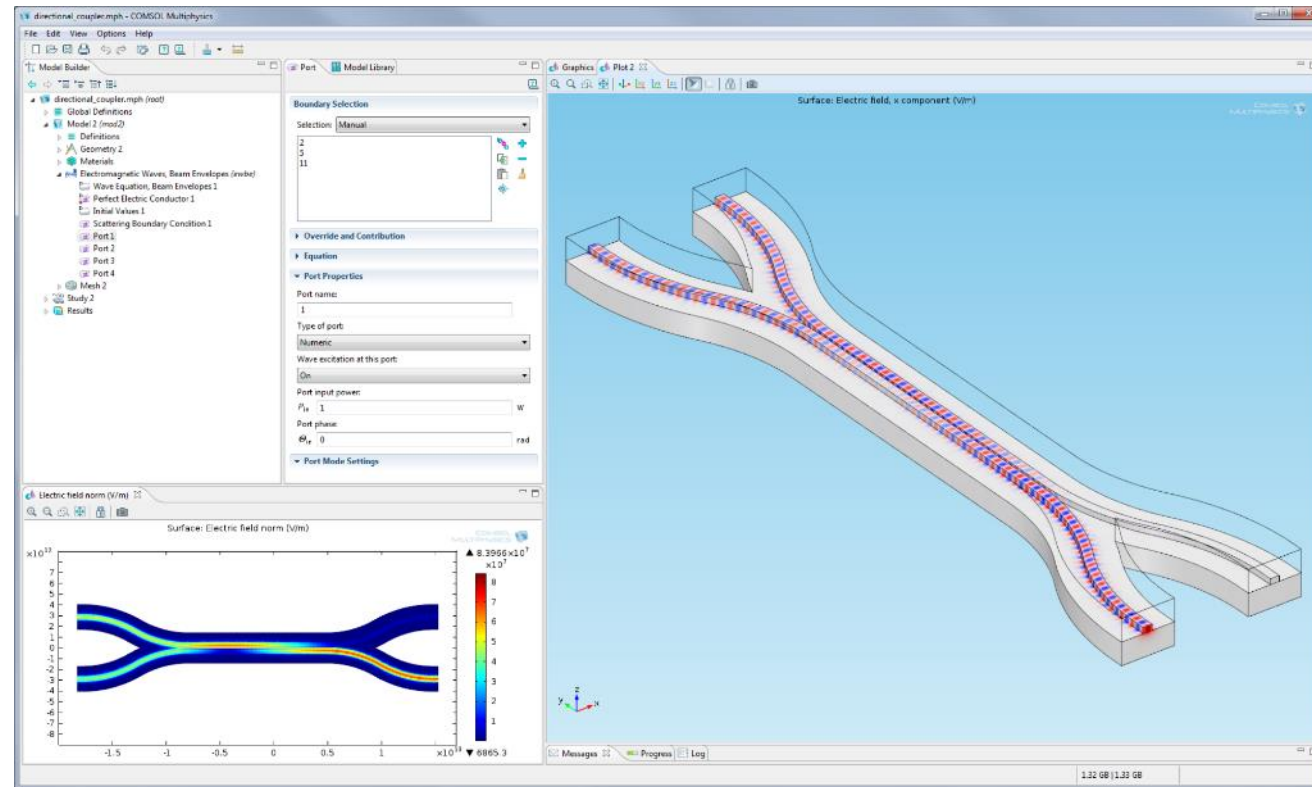


Figure 12: Waveguide coupler, from COMSOL Multiphysics.

GRATING-ASSISTED DIRECTIONAL COUPLER

- Grating helps to match propagation constants and induces power transfer for specific input wavelengths.
- Grating period $\Lambda = 2\pi/|\beta_1 - \beta_2|$. Typically, $\Lambda \sim 10 \mu\text{m}$ (a long-period grating).
- A short-period grating is used if light is launched in opposite directions.

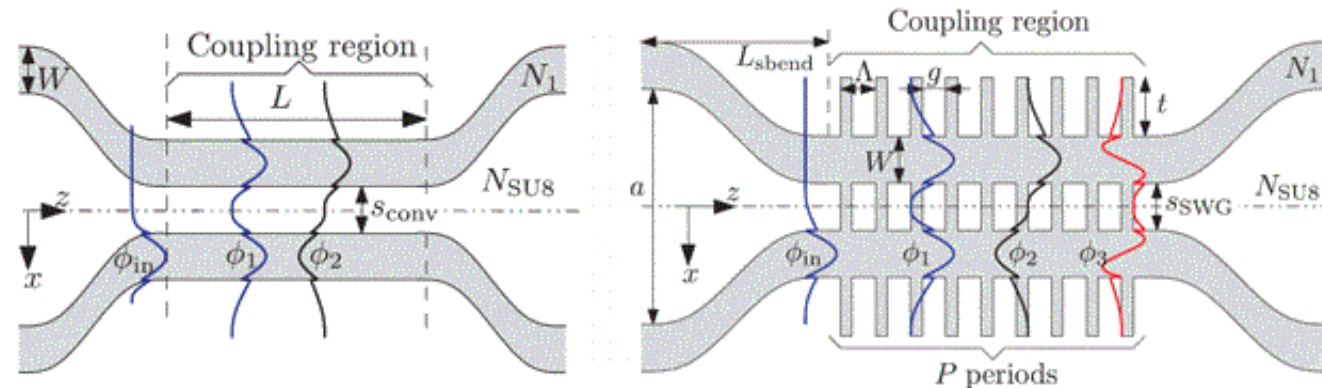


Figure 13: Grating Assisted Directional Coupler. R. Halir et al. Optics Express, 20(12), pp. 13470-13477 (2012).

MACH-ZEHNDER SWITCHES

- Two arm lengths are equal in a symmetric MZ interferometer.
- Such a device transfers its input power to the cross port.
- Output can be switched to bar port by inducing a π phase shift in one arm.
- Phase shift can be induced electrically using a thin-film heater (a thin layer of chromium).
- Thermo-optic effect is relatively slow.
- Much faster switching using electro-optic effect in LiNbO_3 .

MACH-ZEHNDER SWITCHES

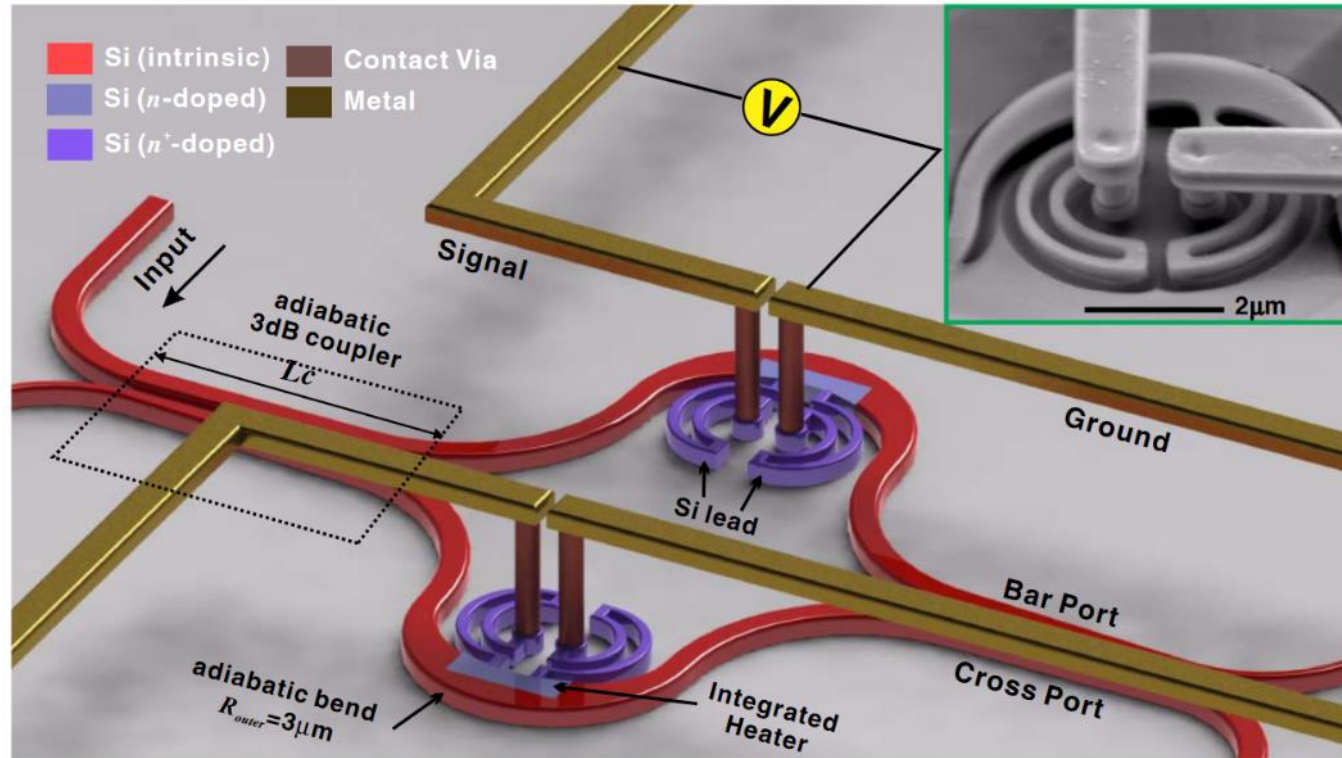


Figure 14: Schematics of broadband thermo-optic switch. Michael R. Watts et al., optics letters, Vol. 38, No. 5 (2013).

MACH-ZEHNDER FILTERS

- An asymmetric MZI acts as an optical filter.
- Its output depends on the frequency ω of incident light when the transfer function is $H(\omega) = \sin(\omega\tau)$. τ is the additional delay in one arm of MZI.
- Such a filter is not sharp enough for applications.
- A cascaded chain of MZI provides narrow band optical filters.
- In a chain of N cascaded MZIs, one has the freedom of adjusting N delays and $N + 1$ splitting ratios.
- This freedom can be used to synthesize optical filters with arbitrary amplitude and phase responses.

MACH-ZEHNDER FILTER

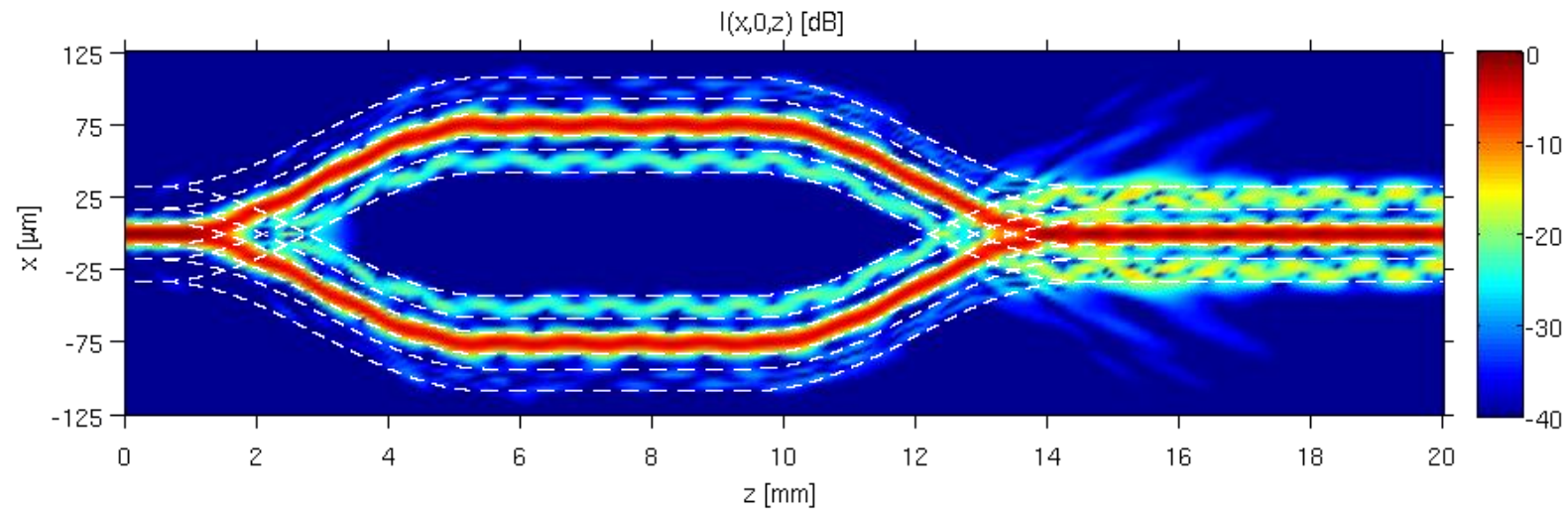


Figure 15: Mach-Zehnder Filter, Beamlab.

CASCADE MACH-ZEHNDER FILTERS

- Transmission through a chain of N MZIs can be calculated with the transfer-matrix approach. In matrix form: $F_{\text{out}}(\omega) = T_{N+1}D_N T_N \cdots D_2 T_2 D_1 T_1 F_{\text{in}}$
- T_m is the transfer matrix and D_m is a diagonal matrix:

$$T_m = \begin{bmatrix} c_m & js_m \\ js_m & c_m \end{bmatrix} \quad D_m = \begin{bmatrix} e^{j\phi_m} & 0 \\ 0 & -e^{j\phi_m} \end{bmatrix}$$

$c_m = \cos(k_m l_m)$ and $s_m = \sin(k_m l_m)$ and $2\phi = \omega\tau_m$

- Simple rule: sum over all possible optical paths. A chain of two cascaded MZIs has four possible paths:

$$t_b(\omega) = jc_1 c_2 s_3 e^{j(\phi_1 + \phi_2)} + jc_1 s_2 s_3 e^{j(\phi_1 - \phi_2)} + js_1 c_2 s_3 e^{j(-\phi_1 + \phi_2)} + js_1 s_2 s_3 e^{-j(\phi_1 + \phi_2)}$$

CASCADE MACH-ZEHNDER FILTERS

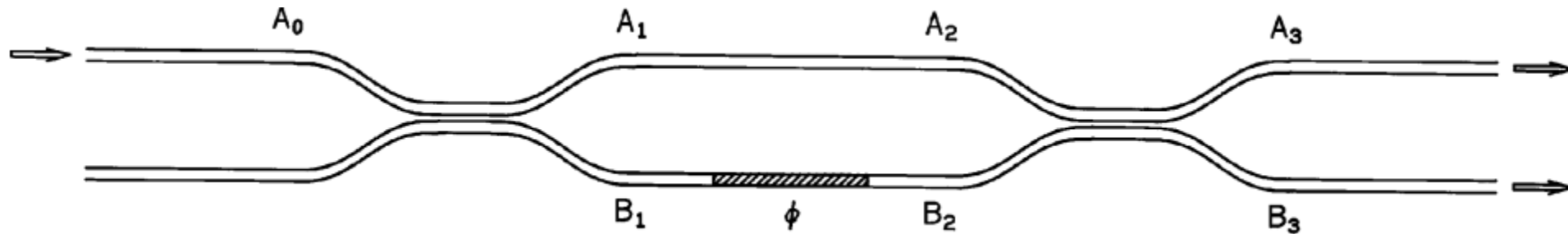


Figure 16: Illustration from Govind P. Agrawal, "Fiber Optic Communication Systems", Page 366.

MULTIMODE INTERFERENCE COUPLERS

- Multimode interference (MMI) couplers are based on the Talbot effect: Self-imaging of objects in a medium exhibiting periodicity.
- Same phenomenon occurs when an input waveguide is connected to a thick central region supporting multiple modes.
- Length of central coupling region is chosen such that optical field is self-imaged and forms an array of identical images at the location of output waveguides.
- Such a device functions as a $1 \times N$ power splitter.

MULTIMODE INTERFERENCE COUPLERS

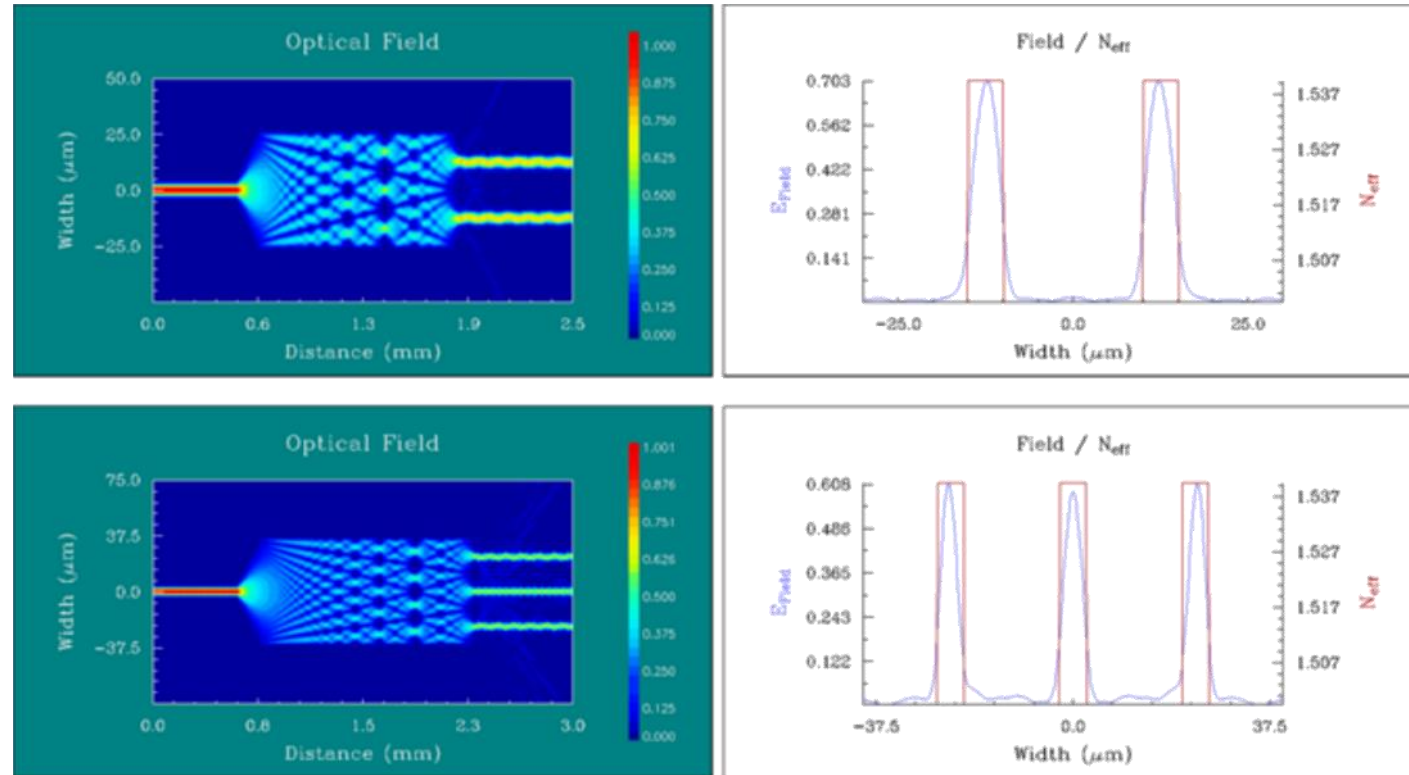


Figure 17: Multimode Interference Couplers, from Opt. Eng. 46(1), 013401, 2007.

MULTIMODE INTERFERENCE COUPLERS

- Expand input field into mode $\phi_m(x)$ as $A(x, z) = \sum C_m \phi_m(x)$.
- Field at a distance z : $A(x, z) = \sum C_m \phi_m(x) e^{j\beta_m z}$.
- Propagation constant β_m for a slab of width W_e : $\beta_m^2 = n_s^2 k_0^2 - p_m^2$, where $p_m = (m + 1)\pi/W_e$.

- Since $p_m \ll k_0$, we can approximate β_m as:

$$\beta_m \approx n_s k_0 - \frac{(m + 1)^2 \pi^2}{2n_s k_0 W_e^2} = \beta_0 - \frac{m(m + 2)\pi}{3L_b}$$

- Beat length - $L_b = \frac{\pi}{\beta_0 - \beta_1} \approx \frac{4n_s W_e^2}{3\lambda}$.
- Multiple images of input can form for $L < 3L_b$.

STAR COUPLERS

- Some applications make use of $N \times M$ couplers designed with N input and M output ports. Such couplers are known as star couplers.

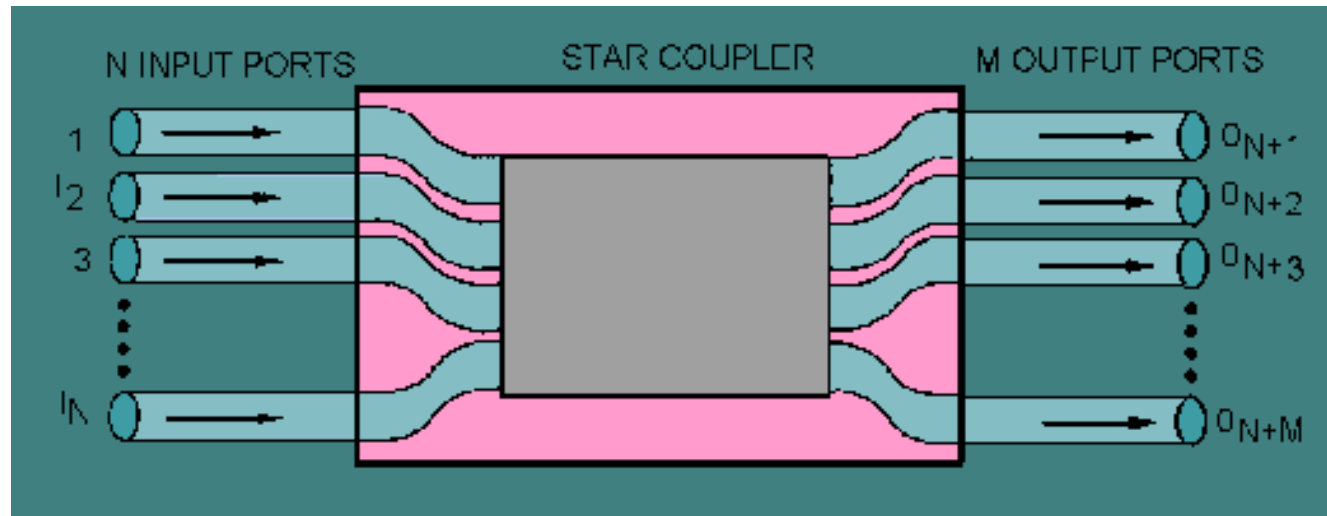


Figure 18: star couplers.

STAR COUPLERS

- They can be made by combining multiple 3-dB couplers. For example, A 8×8 star coupler requires twelve 3-dB couplers. The device design becomes too cumbersome for larger ports.
- Compact star couplers can be made using planar waveguides. Input and output waveguides connect to a central region. Optical field diffracts freely inside central region.
- Waveguides are arranged to have a constant angular separation. Input and output boundaries of central slab form arcs that are centered at two focal points with a radius equal to focal distance. Dummy waveguides added near the edges to ensure a large periodic array.

STAR COUPLERS

- An infinite array of coupled waveguides supports supermodes in the form of Bloch functions.
- Optical field associated with a supermode: $\psi(x, k_x) = \sum_m F(x - ma)e^{jmk_x a}$.
- $F(x)$ is the mode profile and a is the period of array.
- k_x is restricted to the first Brillouin zone: $-\pi/a < k_x < \pi/a$
- Light launched into one waveguide excites all supermodes within the first Brillouin zone.
- As waveguides approach central slab, $\psi(x, k_x)$ evolves into a freely propagating wave with a curved wavefront.
- $\theta \approx k_x/\beta_s$ where β_s is the propagation constant in the slab.

STAR COUPLERS

- Maximum value of this angle: $\theta_{BZ} \approx \frac{k_x^{max}}{\beta_s} = \frac{\pi}{\beta_s a}$.
- Star coupler is designed such that all N waveguides are within illuminated region: $Na/R = 2\theta_{BZ}$, where R is focal distance.
- With this arrangement, optical power entering from any input waveguide is divided equally among N output waveguides.
- Silica-on-silicon technology is often used for star couplers.

H.W.

The task

- 1) In a Y junction: explain the fundamental difference between the S bends and Y bends.
- 2) Define the transfer function in MZ filters.
- 3) What is the relation between the Talbot effect and Fresnel diffraction (The Nature Physics website has a Talbot carpet in its header :)?
- 4) Why does an infinite array of coupled waveguides support supermodes in the form of Bloch functions?

BIBLIOGRAPHY

- [1] Katiyi, A., Karabchevsky, A., 'Figure of merit of all-dielectric waveguide structures for absorption overtone spectroscopy'. *Lightwave Technology*, 35:14, 2902 - 2908 (2017).
- [2] M. N. Weiss, and R. Srivastava. 'Determination of ion-exchanged channel waveguide profile parameters by mode-index measurements'. *Applied optics* 34.3 (1995).
- [3] Karabchevsky, A, Katiyi, A., Ang, A. S., Hazan, A., 'On-chip nanophotonics and future challenges'. *Nanophotonics, Invited Review*, 9(12), 3733-3753 (2020).
- [4] Karabchevsky, A., Sheintop, U., Katiyi, A., 'Overtone Spectroscopy for Sensing - Recent Advances and Perspectives', *ACS Sensors*, 7(10), 2797-2803 (2022).
- [5] A. Katiyi and A. Karabchevsky, 'Passive and active materials for advanced photonic integrated circuitry in visible and near-infrared'. Book "Photonic Materials" - *Encyclopedia of Materials* (Elsevier) ed E. Purushottam Chakraborty 2020.